Measurements of Mode I Interlaminar Properties of Carbon Fiber Reinforced Polymers using Digital Image Correlation

Matthias Merzkirch[1, a *], Louise Ahure Powell[1,2, b] and Tim Foecke[1,2, c]

[1]NIST Center for Automotive Lightweighting (NCAL), National Institute of Standards and Technology, Gaithersburg, MD 20899-8557, USA

[2]Department of Materials Science and Engineering, University of Maryland, College Park, MD, USA

[a]matthias.merzkirch@nist.gov, [b]louise.ahurepowell@nist.gov, [c]timothy.foecke@nist.gov

Keywords: R-curve, crack tip tracking, fracture toughness, DIC, DCB, Standards, Metrology, PMC

Abstract. Numerical models based on cohesive zones are usually used to model and simulate the mechanical behavior of laminated carbon fiber reinforced polymers (CFRP) in automotive and aerospace applications and require different interlaminar properties. The current work focuses on determining the interlaminar fracture toughness (G_{IC}) under Mode I loading of a double cantilever beam (DCB) specimen of unidirectional CFRP, serving as prototypical material. The novelty of this investigation is the improvement of the testing methodology by introducing digital image correlation (DIC) as an extensometer and this tool allows for crack growth measurement, phenomenological visualization and quantification of various material responses to Mode I loading. Multiple methodologies from different international standards and other common techniques are compared for the determination of the evolution of G_{IC} as crack resistance curves (R-curves). The primarily metrological sources of uncertainty, in contrast to material specific related uncertainties, are discussed through a simple sensitivity analysis. Additionally, the current work offers a detailed insight into the constraints and assumptions to allow exploration of different methods for the determination of material properties using the DIC measured data. The main aim is an improvement of the measurement technique and an increase in the reliability of measured data during static testing, in advance of future rate dependent testing for crashworthiness simulations.

Introduction

Motivation. The use of polymer composites for structural components in the automotive and aerospace sectors requires a detailed and robust understanding of the deformation and damage behavior under different loading conditions and loading rates in order to model and simulate the mechanical behavior. Laminar carbon fiber reinforced polymers (CFRP) consist of different layers that all contribute to the mechanical performance of the product. The mechanical interlaminar properties are affected by the volume fraction, the architecture and orientation of the single constituents [1], as well as parameters of the production process. Numerical models based on cohesive zones [2] are usually used to describe the interlaminar behavior. These models have inputs for different interlaminar properties, including energy, stress and displacement related parameters, to be determined under Mode I, Mode II and mixed Mode loading conditions.

Standards and Methods for Determination of the Fracture Toughness (G_I). The unidirectionally-reinforced double cantilever beam (DCB) test under Mode I loading is used as a comparative quality control for produced laminates. It gives insights into a variety of methods to determine the energy needed to advance a crack over a width (w) within a specimen of thickness (h). The overall crack length (a) corresponds to the horizontal [3,4] distance from the point of load introduction to the tip of the growing crack (a_i), including the length of the precrack (a_0). Various methods exist to determine the fracture toughness; six commonly used methods are reviewed and compared here.

The Area method [1,5,6], which does not provide an initiation value [7] includes the (irreversible) work determined from force (F)-displacement (δ) curves, needed for crack growth:

$$G_{IC}^{Area} = \frac{\int_{irrev} F \cdot d\delta}{w \cdot a_i}. \quad (1)$$

The Simple Beam (SB) theory method [1,6,7] will overestimate G_{IC}, due to the oversimplification of assuming built-in conditions at the delamination front [6,7]:

$$G_{CI}^{SB} = \frac{3}{2}\frac{F \cdot \delta}{w \cdot a}. \quad (2)$$

In order to compensate the former assumption, that the deflection at the cantilever beam root is zero [6], the Modified Beam Theory (MBT [7]) or Corrected Beam Theory (CBT [3]) method [1,6] includes a shift (Δ) of the crack length to zero the third root of the compliance (δ/F) at a = 0 mm [6]:

$$G_{IC}^{MBT} = \frac{3}{2}\frac{F \cdot \delta}{w \cdot \left(a + |\Delta|\right)}. \quad (3)$$

This correction also allows for a determination of the flexural modulus [6,7]:

$$E_{if} = \frac{64 \cdot \left(a + |\Delta|\right)^3 \cdot F}{\delta \cdot w \cdot h^3}. \quad (4)$$

The Compliance Calibration (CC [7]) method [1] includes the slope (n) of the relationship between the logarithm of the compliance and the logarithm of the crack length:

$$G_{IC}^{CC} = \frac{n \cdot F \cdot \delta}{2 \cdot w \cdot a}. \quad (5)$$

The Modified Compliance Calibration (MCC [3, 7]) method [4] includes the slope (A_1) between (a/h) and the third root of the compliance (C):

$$G_{IC}^{MCC} = \frac{3}{2}\frac{F^2 \cdot C^{2/3}}{A_1 \cdot w \cdot h}. \quad (6)$$

A non-standardized procedure, with the advantage of requiring fewer measured inputs (i.e., no need to measure the crack length) is the Pure Compliance (PC) method [6]:

$$G_{IC}^{PC} \cong \frac{12 \cdot F^2 \cdot a^2}{E_1 \cdot w^2 \cdot \left(h/2\right)^3}. \quad (7)$$

This approach is based on neglecting the shear effects (for a/h > 10 [7]). The crack length can be determined via the compliance, but requires the value of the tensile modulus (E_1) in the 0° direction [6], typically from a separate uniaxial test:

$$C = \frac{\delta}{F} \cong \frac{8 \cdot a^3}{E_1 \cdot w \cdot \left(h/2\right)^3}. \quad (8)$$

Metrological Development and Improvement with DIC. The novelty of the current investigation is the improvement of the testing setup metrology by introducing digital image correlation (DIC) as an extensometer (δ), a tool for crack growth measurement (a_i) and through phenomenological visualization and quantification of different full-field behaviors (e.g., absolute displacements, strains and rotations) under Mode I loading. Additionally, DIC allows for a detailed insight into the constraints and assumptions of different methods, with the aim of improving the measurements.

Experimental Details

Materials and Specimen Geometry. The reference material investigated in this work was produced by DOW Chemical Company. The unidirectional carbon fiber (DowAksa A-42, 24K) reinforced epoxy prepregs were formed by sheet molding compound (SMC) process. Thereby, nominally 12 prepreg layers with a reported reinforcing volume fraction of 50 % were stacked up, resulting in a thickness of the cured laminate sheet material of about 2.3 mm.

A standardized rectangular DCB specimen, with the dimensions: l x w = 120 mm x 20 mm (including a 50 mm long and 55 µm thick Teflon film symmetrically inserted during production from one end to act as a precrack) was cut with a waterjet cutting system MAXIEM 1515 from Omax Corporation. Preliminary studies were conducted to determine the effect of the waterjet cutting parameters (i.e., nozzle diameter, pressure, speed, abrasive grit size, etc.) and optimize the cutting conditions to ensure minimal fabrication damage in the test specimen. Both the specimen and hinge surfaces were prepared before applying 3M Scotch-Weld Low-Odor Acrylic Adhesive DP810 to attach the hinges onto the specimen.

Experimental Setup with DIC Settings. The test was carried out on an Instron electromechanical Universal Testing System, Model 4465 with a maximum load capacity of 5 kN. The displacement-controlled test was conducted at a rate of 1 mm/min consistent with [3,4,7].

For DIC measurement, two 5-megapixel CCD cameras (2448 pixel (px) x 2048 px Point Grey) and Sigma 105 mm lenses (Nikon) were situated perpendicular to one side of the specimen. One edge side was prepared for DIC measurement with matte white primer, followed by applying matte black protective enamel spray paint (both Rust-Oleum) to create a random pattern by an overspray method. For data acquisition (with an image acquisition rate of 0.5 s^{-1}), Vic-Snap image acquisition from Correlated Solutions was used. Fig. 1 shows the camera field of view (FOV) and the DIC area of interest (AOI, colored area) used to determine the opening at the load introduction points, Fig. 1(a), and for crack growth measurements, Fig. 1(b). The length of the precrack from the center of the pin of the hinge [7] to the tip of the precrack was 40.08 mm ± 0.2 mm.

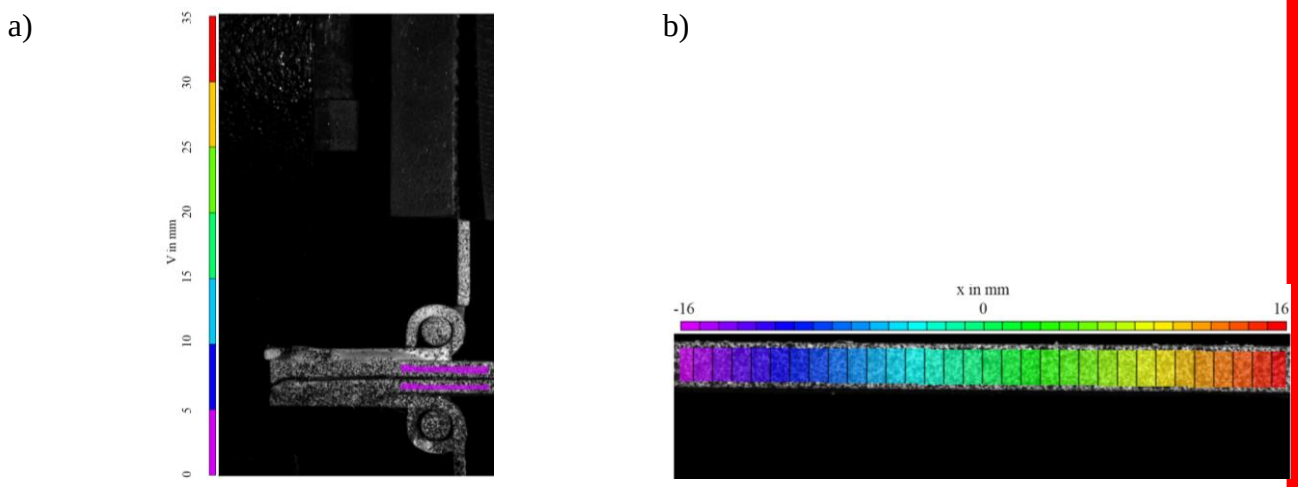

Fig. 1: DIC monitoring for a) extensometer (horizontally cropped image), magnification ≈ 58 px/mm, pixel size ≈ 17 µm, subset size (controls the area of the image that is used to track the displacement between images) = 29 px, step size = 7 px b) crack growth (vertically cropped image), magnification ≈ 76 px/mm, pixel size ≈ 13 µm, subset size = 21 px, step size = 5 px.

Results and Discussion

Results. Fig. 2(a) depicts the force-displacement curves measured via crosshead displacement and DIC during tensile loading of a DCB specimen, showing only a slight difference presumably to machine compliance ($C_{crosshead}$ = 0.1613 mm/N, C_{DIC} = 0.1610 mm/N). It is important that hinge-specimen interfaces located as shown in Fig. 1(a) in order to avoid a stiffening of the bending cantilevers portion of the specimen. Fig. 2(b) shows the use of DIC crack tip tracking via post-test method using the quality of correlation (sigma), defining a threshold value for the match; high sigma value corresponds to high uncertainty. In the vicinity of the crack surfaces and the crack tip some subsets lose correlation and these sections of the AOI no longer show data (see Fig. 2(b)).

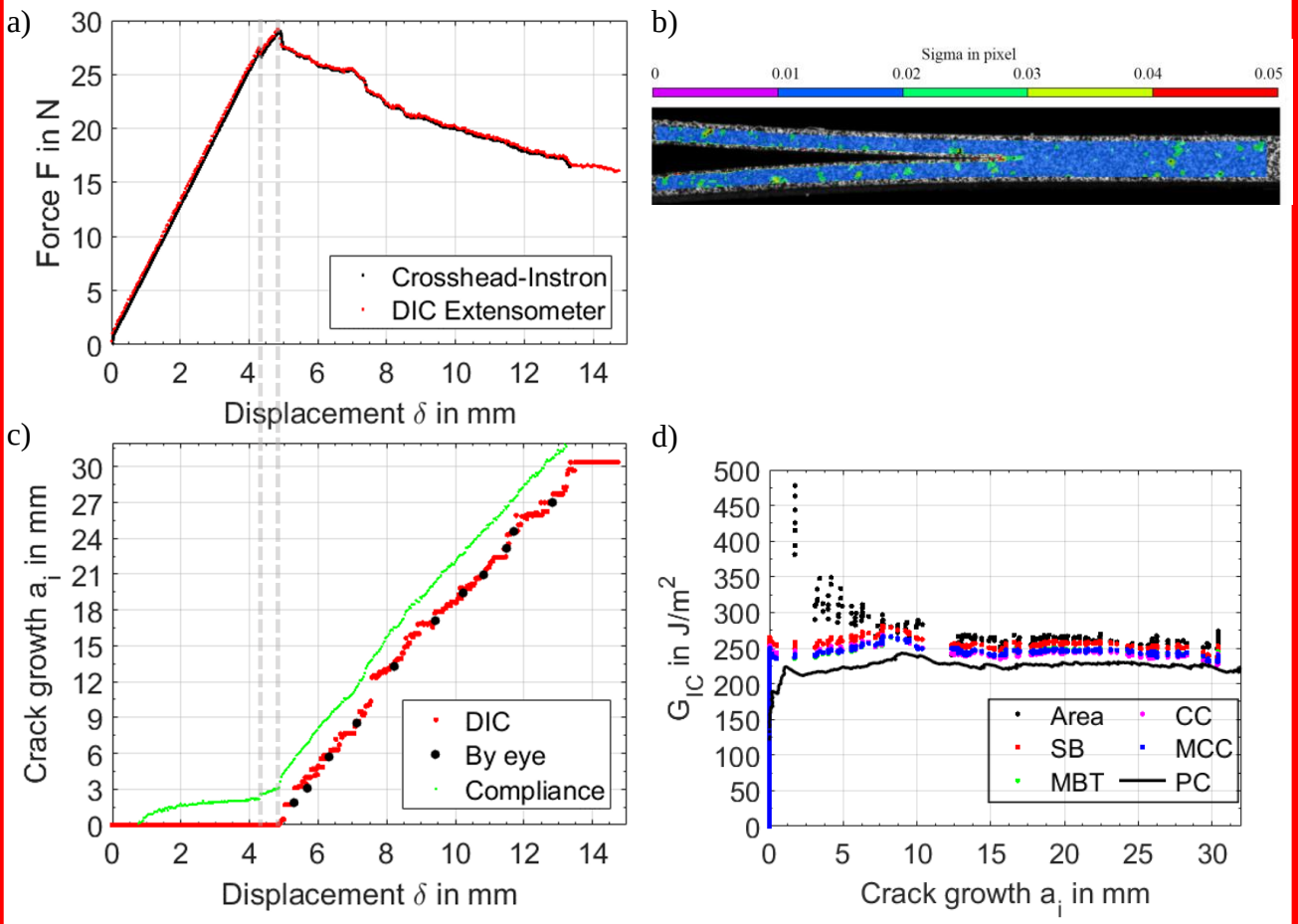

Fig. 2: a) Force-displacement curves, b) representative DIC image depicting sigma, c) evolution of crack growth by various methods d) R-curves of different methods using DIC to measure δ.

By following a threshold value of sigma (DIC) the crack path may be determined in absolute coordinates and the evolution of the crack growth, shown in Fig. 2(c), can be determined. A comparison with selected crack lengths measured from the image by eye show good agreement (Fig. 2(c)). In direct comparison to the force-displacement curve, crack growth via DIC can be determined starting at a displacement of less than 5 mm, at the force maximum where crack growth is accompanied by a steady decrease in force. Crack length determination via the compliance method (Eq. 8) results in an earlier crack propagation ($\delta \approx 4.3$ mm), whereas the initial crack length is overestimated by about 2 mm (offset of green data at $\delta < 4.5$ mm in Fig. 2(c) was corrected for further analysis). According to [3,7] a correction factor is needed if $\delta/a > 0.4$ due to bending of the DCB specimen. For the current test, at the maximum measured crack length, $\delta/a \approx 0.2$ suggest the deformations are small and no correction is needed.

Fig. 2(d) shows the evolution of the fracture toughness G_{IC} over crack growth a_i (up to a maximum of about 30 mm, which corresponds to the AOI) as a crack resistance R-curve for the

different methods described in the introduction and determined with the displacement and crack growth measurement via DIC (except for PC method). Since the initiation value can be influenced by the specimen production process of placing a Teflon film between the plies [8], no conclusions will be drawn at this point. It can be seen that all methods presented show crack propagation bounded by the area method (maximum) and the pure compliance method (minimum) predictions.

DIC also allows for phenomenological visualization and quantification of different effects, Fig. 3(a) shows high vertical strains ε_{yy} of > 5 % in the vicinity of the crack tip. The high strains along the crack surfaces are partially artifacts of subset decorrelation.

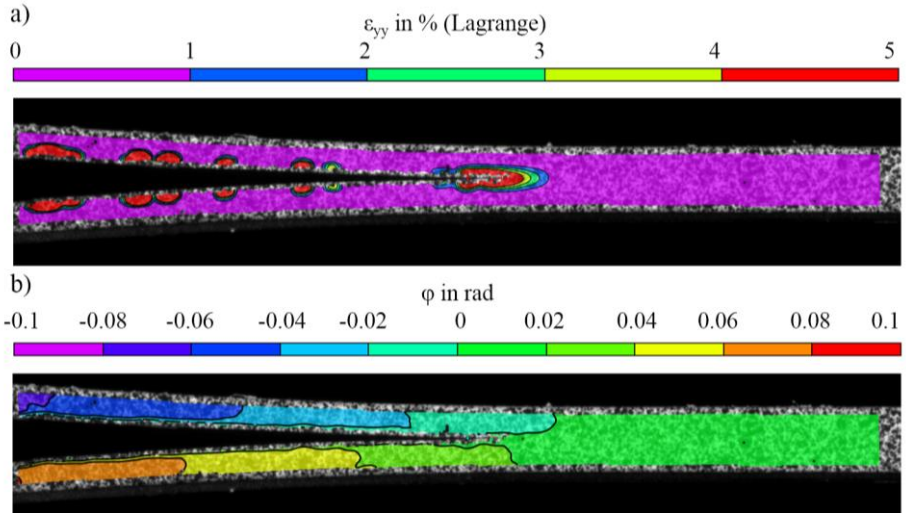

Fig. 3: DIC contour plots, at a_i = 17.86 mm a) ε_{yy} (vertical) strains b) in plane rotations φ.

Fig. 3(b) depicts the rotational effects in the form of a contour plot with iso-lines. As stated in [6] and [7], rotations are possible at the delamination front and are seen here to be between -0.02 rad (≈ 1.15° CW) and 0.02 rad (≈ 1.15° CCW), decreasing in front of the crack tip.

Sensitivity Analysis and Metrological Sources of Uncertainty. Fig. 4(a) compares the fracture toughness for crack propagation $G_{IC,prop}$ (average of values between a_i = 10 mm to 30 mm in Fig. 2(d)) with error bars from maximum to minimum values for all the methods. The influence of the compliance of the crosshead is seen in the difference between the δ_{DIC} and $\delta_{crosshead}$ results. The area method is a maximum, comparable to the simple beam method, and shows the highest fluctuations during crack propagation (see also Fig. 2(d)). The crack growth a_i used for each method was the DIC measured value, except where a_i+1 mm was used to demonstrate the sensitivity to that parameter and PC that only uses displacement δ.

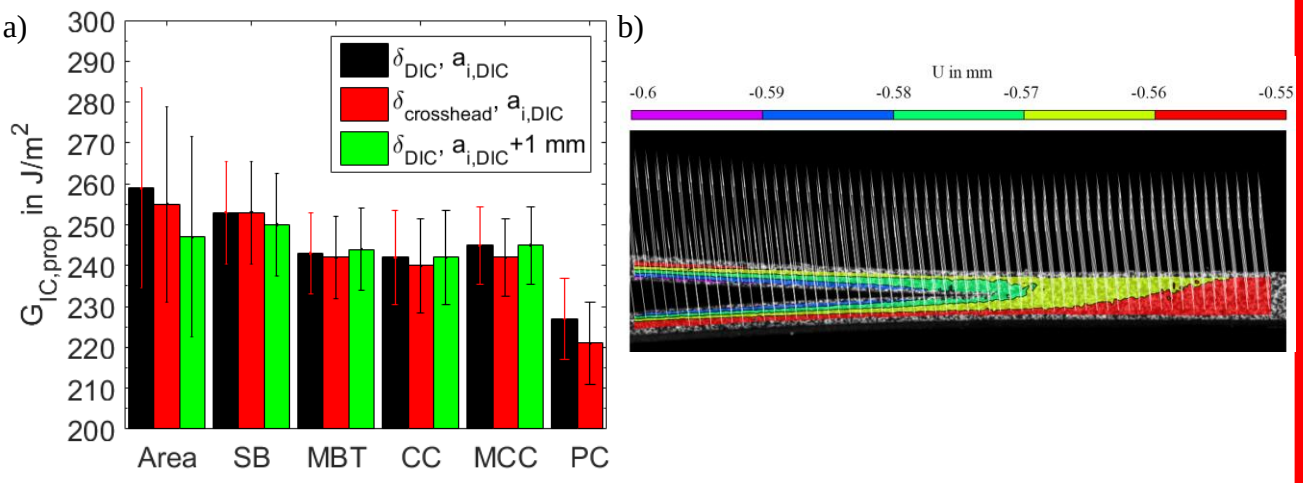

Fig. 4: a) Comparison of different methods and sensitivity analysis for crack propagation b) DIC image showing the horizontal shift (U, negative to the left) of the specimen (at a_i = 17.86 mm).

Since the standardized compliance methods MBT, CC and MCC include a correction of the crack length, the values obtained show barely any difference either via the change in compliance, or via the implementation of an artificial change of the crack length.

DIC investigations also allow for visualization of rigid body motion, as shown in Fig. 4(b), that will affect crack growth measurement. This shift of the specimen towards the load application point results from bending of both cantilever arms (arrows in Fig. 4(b)), but within the limits of [3,7] (see δ/a calculation). Additionally, the contour plot depicts the horizontal shift towards the load introduction point, that leads to a reduction in the measured overall crack length. For the DIC image shown, the measured crack length is a = 57.95 mm including a reduction, due to a horizontal shift of about 0.57 mm towards the loading point.

Other sources of uncertainty that are related to material/production include the homogeneity of the precrack over the specimen width, Fig. 5(a) left. Furthermore, the inhomogeneous fiber concentration within the prepregs and the subsequent stacking and pressurized curing can be seen as a waviness in the precracked and cracked section (Fig. 5(a) and in the cross section in Fig. 5(b)). Most techniques for crack tip tracking do not capture the inhomogeneous crack growth over width, which can be seen at the delamination front at the end of the test (right side of Fig. 5(a)).

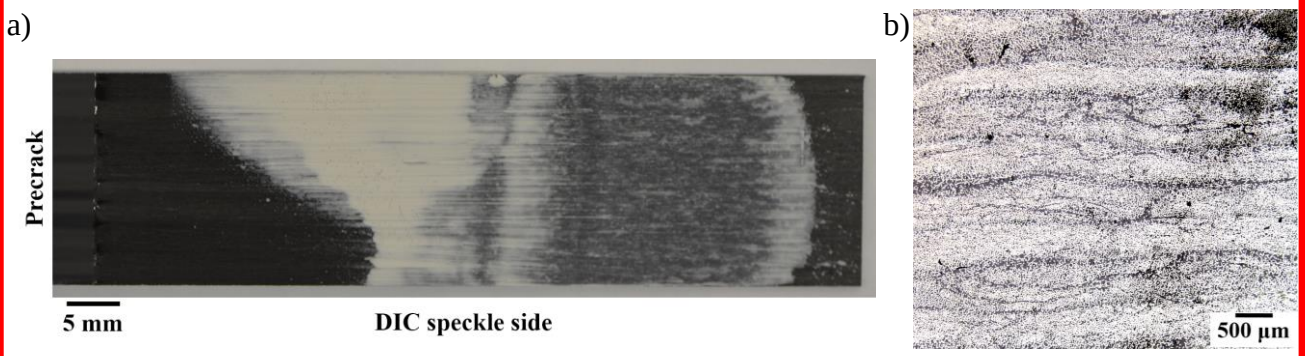

Fig. 5: a) Example fractography (crack growth in horizontal direction, w along vertical direction) of a DCB specimen (crack surfaces have been painted to visualize inhomogeneous crack growth) b) Representative cross section (w along horizontal direction, h along vertical direction).

In order to understand the corrections of the crack length needed for determining fracture toughness according to the standardized compliance related methods, Fig. 6(a) visualizes the deformation (representative for one cantilever arm) behavior for multiple DIC images in the vicinity of the crack tip via Crack Opening Displacement (COD) measurements, including the point of no deformation and the opening at the crack tip.

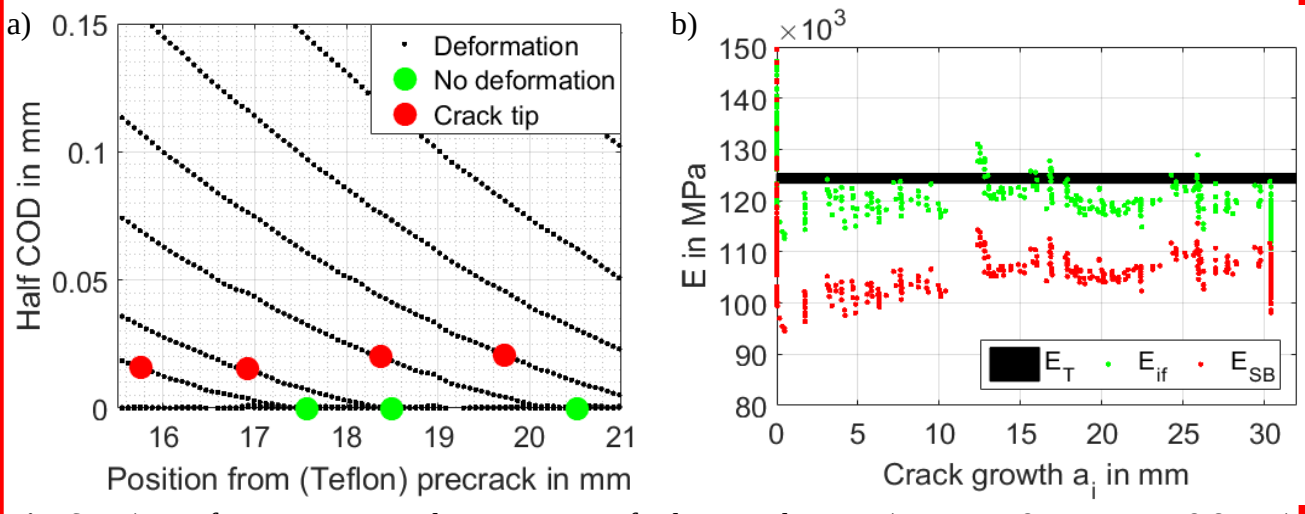

Fig. 6: a) Deformations in the vicinity of the crack tip (a = 55.9 mm to 59.8 mm) b) Comparison of the evolution of the flexural moduli (E_{if}, E_{SB}) to the tensile modulus (E_T).

A mechanical approach for understanding the correction of the crack length is given by the second derivative of the deflection of a single cantilever (δ_{sc}) of length L due to a bending moment $M = F \cdot L$, acting at the root of the cantilever beam where $\delta_{sc} = 0$:

$$\delta''_{sc}(x) = -\frac{F \cdot (L - x)}{E \cdot I}. \tag{9}$$

By integrating twice, the deflection δ of one cantilever arm can be expressed by:

$$\delta_{sc}(x) = \frac{1}{6} \cdot \frac{F}{E \cdot I} \cdot x^3 - \frac{1}{2} \cdot \frac{F}{E \cdot I} \cdot x^2 \cdot L + C_1 \cdot x + C_2. \tag{10}$$

Since at $x = 0$ the deflection is zero (green dots in Fig. 6(a)) and the rotation is zero (see also Fig. 3(b)) Eq. 10 can be simplified to the first two terms. For $x = L$, Eq. 10 represents the simple beam theory. At $x = (L\text{-}a)$ (at the crack tip) the deflection is equal to the crack tip opening displacement (red dots in Fig. 6(a)). Fig. 6(a) visualizes that the deflection at the root of the cantilever is not zero [6] (material is still deformed in front of the crack tip) and that the correction factor Δ, used in equations (3) and (4), leads to an overestimation of the real crack length.

By including the correction factor Δ = 2.45 mm in Eq. 4, the calculated flexural modulus (E_{if} = 121 GPa ± 8 GPa) is greater than the modulus from simple beam theory (E_{SB} = 107 GPa), see range 10 mm to 30 mm in Fig. 6(b). In direct comparison to the tensile (chord) modulus, which was determined to be 124 GPa ± 1 GPa in the 0° direction by a uniaxial test, a good agreement can be achieved via the corrected modulus.

By using the points of no deformation (green dots in Fig. 6(a)) with the simple beam theory, a comparable flexural modulus of 118 GPa ± 4 GPa and an average fracture toughness of about 246 J/m^2 can be determined. By using the points of no deformation with the area method a fracture toughness of about 236 J/m^2 can be determined. Both methods show comparable fracture toughness values to the MBT-compliance method (243 J/m^2), see Fig. 4(a).

Summary and Conclusions

The current work focused on metrology-based improvements and the implementation of DIC in order to allow a detailed investigation and determination of the fracture toughness under Mode I loading conditions of a unidirectionally CFRP double cantilever beam.

The method presented for crack tip tracking by DIC (to be published) is in good agreement with pure visual crack length determination, but statements about the accuracy ([3,4] require ± 0.5 mm) should be the focus of future investigations. Furthermore, this method allows for the determination of crack growth rates for different loading rates. The determination of crack growth is limited to about 30 mm with the current camera setup (based on FOV), but could easily be extended by e.g. using multiple cameras in order to satisfy the suggested investigation of the crack length over a minimum of 50 mm [7].

From the comparison of standardized and non-standardized methods for determination of the fracture toughness, the area method (followed by simple beam theory) shows the highest values and the pure compliance method shows the lowest values (in good agreement with [6]). The advantage of the latter method is that a minimum of measured input is needed at high loading rates, although the rate sensitivity has to be investigated. The standardized compliance methods barely show a sensitivity either to a change in crack growth or displacement measurement, as already confirmed by [1]. The crack length correction could be visualized with DIC measured COD, noting that the area method is the only method relating to the real crack length.

The comparison of the methods aimed for an increase in the reliability of the measured data as a future output for rate-dependent testing for crashworthiness simulations. The current suggested displacement rates lie between 1 mm/min [3,4,7] and 10 mm/min [5]. In order to understand the use

of rate-dependent data, it should be investigated how strain rates are applied since displacement rates do not represent a material related property. A solution could be found by combining either the critical vertical strain or deformation at the crack tip with the crack growth rate.

Future work could also include a more materials science based approach (based on underlying material properties) to get detailed knowledge about the sources of the fluctuations (e.g., wavy plies, stitched fiber bundles, etc. [1]). In order to simplify the production process of precracked specimens, waterjet cut notches in CFRP plaques, that are already being successfully produced at NCAL, instead of using Teflon inserts, could be investigated concerning crack initiation and propagation.

Additionally, DIC could be a favorable tool for detailed insights into the deformation and delamination behavior of non-unidirectional (e.g., woven) composites. Beside this, the current method could be extended to adhesives, that are also currently a focus area for investigation within the automotive sector, as well as additive manufactured materials.

Future work under Mode I loading conditions will focus on analytical mechanics based models, where the COD tool will be used for a more precise examination of fracture toughness values in the vicinity of the crack tip. Furthermore, analytical models applied to the area between the opening at the crack tip and the point of no deformation (representing the material behavior) could potentially be exploited to determine the interlaminar normal strength.

Acknowledgement

This work was carried out under the ICME Development of Carbon Fiber Composites for Lightweight Vehicles project directed by Ford and funded by the U.S. Department of Energy under contract number DE-EE0006867. Thanks to Dave Pitchure for waterjet cutting the DCB specimens.

Disclaimer

Certain commercial equipment, instruments, or materials are identified in this paper to foster understanding. Such identification does not imply recommendation or endorsement by the National Institute of Standards and Technology.

References

[1] C. Starke, W. Beckert, B. Lauke, Characterization of the delamination behaviour of composites under mode I- and mode II - loading, Materialwiss. Werkstofftech. 27 (1996) 80-89.

[2] K. Song, C. G. Dávila, C. A. Rose, Guidelines and parameter selection for the simulation of progressive delamination, Abaqus Users' Conference (2008) 1-15.

[3] ISO 15024:2001 (E), Fibre-reinforced plastic composites - Determination of mode I interlaminar fracture toughness, G_{IC}, for unidirectionally reinforced materials, International Standard (2001).

[4] JSA JIS K 7086 ERTA, Testing methods for interlaminar fracture toughness of carbon fibre reinforced plastics, Japanese Industrial Standard, (1997) 1-20.

[5] EN 6033, DIN EN 6033, Aerospace series - Carbon fibre reinforced plastics - Test method - Determination of interlaminar fracture toughness energy - Mode I - G_{IC}, European Standard, (2015).

[6] S. Hashemi, A.J. Kinloch, J.G. Williams, Correction needed in double-cantilever beam tests for assessing the interlaminar failure of fibre composites, J. Mater. Sci. Lett. 8 (1989) 125-129.

[7] ASTM D5528-13, Standard test method for mode I interlaminar fracture toughness of unidirectional fiber-reinforced polymer matrix composites, ASTM International, (2013).

[8] A. Beehag, L. Ye., Consolidation and interlaminar fracture properties of unidirectional commingled CF/PEEK composites, J. Thermoplast. Compos. Mater. 9 (1996) 129-150.